# Halloysite nanotube blended nanocomposite ultrafiltration membranes for reactive dye removal

Başak Keskin, Meltem Ağtaş, Türkan Ormancı-Acar, Türker Türken, Derya Y. İmer, Serkan Ünal, Yusuf Z. Menceloğlu, Tuğba Uçar-Demir and İsmail Koyuncu

## ABSTRACT

In this paper, ultrafiltration (UF) flat sheet membranes were manufactured by introducing two diverse halloysite nanotubes (HNT) size (5 μm and 63 μm) and five different (0, 0.63, 1.88, 3.13, 6.30 wt %) ratios by wet phase inversion. Some characterization methods which are contact angle, zeta potential, viscosity, scanning electron microscopy (SEM) and Young's modulus measurements were used for ultrafiltration membranes. Synthetic dye waters which were Setazol Red and Reactive Orange were used for filtration performance tests. These dye solutions were filtered in three different pH conditions and three different temperature conditions for pH and temperature resistance to understand how flux and removal efficiency change. The best water permeability results were obtained as 190.5 LMH and 192 LMH, for halloysite nanotubes (HNT) sizes of 5 μm and 63 μm respectively. The best water and dye performance of UF membrane contains 1.88% w/w ratio of HNT, which showed increased water flux and dye flux of membranes according to different HNT concentrations including ultrafiltration membranes.

**Key words** | dye rejection, flat-sheet membrane, halloysite nanotubes, ultrafiltration membrane

## HIGHLIGHTS

- Ultrafiltration membranes were fabricated by introducing halloysite nanotubes received from two different batches by wet phase inversion method and six different ratios. We examined effects of different pH and temperature on membranes.
- Flux and dye removal efficiency increased when halloysite nanotubes were used in certain concentrations. Mechanical stabilities of the fabricated membranes were discussed.

## GRAPHICAL ABSTRACT

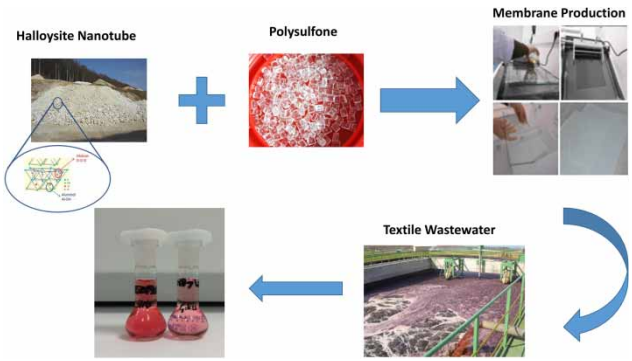


**Başak Keskin**
**Meltem Ağtaş**
**Derya Y. İmer**
**İsmail Koyuncu** (corresponding author)
Environmental Engineering Department,
Istanbul Technical University,
Maslak, 34469, Istanbul,
Turkey
E-mail: *koyuncu@itu.edu.tr*

**Başak Keskin**
**Meltem Ağtaş**
**Türker Türken**
**İsmail Koyuncu**
National Research Center on Membrane Technologies,
Istanbul Technical University,
Maslak, 34469, Istanbul,
Turkey

**Türkan Ormancı-Acar**
Faculty of Engineering, Department of Environmental Engineering,
Istanbul University-Cerrahpaşa,
İstanbul,
Turkey

**Serkan Ünal**
**Yusuf Z. Menceloğlu**
Sabanci University Nanotechnology Research and Application Center,
34956, Tuzla,
Turkey

**Tuğba Uçar-Demir**
ESAN Eczacibasi,
34956, Istanbul,
Turkey

doi: 10.2166/wst.2020.573

## INTRODUCTION

As a result of population growth in the coming years, the amount of water consumed will increase. Limited water resources can be conserved by using treated wastewater. It has to help the industries that consume a lot of water to protect their water resources. The textile, food and steel industries are water-intensive industries (Dilaver *et al.* 2018). For example, China, the largest textile manufacturer, suffers from severe water pollution from dyeing and printing in textile mills (Zhang *et al.* 2014). Necessary studies should be carried out to reduce the water use of this industry or to increase the water resources used. As a result of the various processes, the wastewater with different properties released during the production of textile material is discharged from the treatment plant and generates large amounts of wastewater. Membrane technology is one of the best methods in terms of novelty, efficiency and purity for obtaining desired water quality for water reuse. The wastewater characteristics, color, presence of organic pollutants and salinity are the most important parameters that need to be considered for reusing water from industrial wastewater (Baker 2004). Fiber production results in wastewater with high concentrations of dissolved contaminants, a high level of salt and dark color due to complex and polar dyes. In general, wastewater can be treated by biological methods, while textile wastewater cannot be treated by biological methods as they contain color and salt. The quality of the environment where this kind of wastewater is collected deteriorates quickly and ruins other uses of this water. The treatment of dye-containing textile wastewater is gaining more importance, as discharging unproperly treated wastewater having a low dye presence to the environment can affect aquatic life and lead to visual pollution. Many treatment methods have been used for textile dye wastewaters (Koyuncu 2002). For instance, physical and chemical treatments are commonly used for this purpose. But these methods cannot sufficiently meet discharge standards. As a result, legal wastewater discharge limits are tightened every year and wastewater purification has become a huge issue for the textile industry. There are 114 highly polluting leather plants, 250 textile plants and five paper plants in the Ergene Basin in Turkey. As a result of the discharge of the colored and highly basic wastewater from these plants, the Çorlu and Ergene Rivers have started threatening human health, due to their high level of pollution.

In recent years, membrane technology can be a good option for treating textile dye wastewater because narrow pore sizes of membranes can eliminate dye compounds and discharge high-quality effluent (Liu *et al.* 2016). Many studies have been performed for removing dyes with membranes technologies. Mokkapati *et al.* (2015) reported that graphene oxide concentration is very important to understand the capability of dye filtration. Dye filtration capability of polysulfone depends on graphene oxide concentration and also the best removal efficiency of dye was observed with the graphene oxide membrane at 78.26%. Qin *et al.* (2007) treated dye wastewater by using three diverse membranes to remove dyes and the membrane performance is greater than 99% of removal of dye. Zuriaga-Agustí *et al.* (2002) and Ellouze *et al.* (2012) also documented that the membrane system could completely remove the color from textile wastewater.

An ideal membrane for textile dye wastewater treatment should have both high flux and high dye retention rate (Zhang *et al.* 2014). Because of that reason, most of the studies about ultrafiltration membranes in recent years has been focused on improving membranes by using nanoparticles. Nanoparticles are preferred due to their hydrophilic nature and advanced mechanical and structural properties (Celik *et al.* 2011; Turken *et al.* 2015; Crock *et al.* 2017). Polysulfone (PSf) is widely used as polymeric material for the fabrication of microfiltration and ultrafiltration membranes (Choi *et al.* 2006). However, PSf is hydrophobic and it may lead to undesirable membrane fouling of the membrane surface and membrane pores (Song *et al.* 2016). Ultrafiltration membranes are affected by fouling which decreases the permeation rate (Moslehyani *et al.* 2015). While improving filtration performance, it is important to keep in mind the contamination resistance.

Nowadays, it is being proposed to use nanoparticles and nanotubes of hydrotropic substances to improve the specialty of the membranes, such as titanium dioxide ($TiO_2$) (Sotto *et al.* 2011), carbon nanotube (CNT) (Choi *et al.* 2006), multi-wall carbon nanotube (MWCNT) (Sengur-Tasdemir *et al.* 2018) and halloysite nanotubes (HNTs) (Chen *et al.* 2012; Wang *et al.* 2014; Zeng *et al.* 2016a). HNTs are naturally occurring material that have a hollow tubular shape. It is a unique clay mineral which consists of the hydrogen and oxygen double-layer structure (de Paiva *et al.* 2008). HNTs have superior chemical and physical characteristics which are high aspect ratios, high hydrophilicity and having many hydroxyl groups on the surface. Because of its unique properties, HNT was added to prepare

nanocomposite membranes. Chen *et al.* (2012) studied polyethersulfone ultrafiltration (PES UF) membrane which includes halloysite nanotubes sunk into copper ions ($Cu^{2+}$-HNTs/PES). $Cu^{2+}$-HNTs/PES membranes were found to be highly hydrophilic, having high water flux. The mechanical test showed that the addition of $Cu^{2+}$-HNTs affected the increase of the mechanical strength of the membrane. Wang *et al.* (2014) studied the fabrication of PES ultrafiltration hybrid membranes, containing halloysite nanotubes grafted with 2- methacryloyloxyethyl phosphorylcholine (HNTs-MPC) for improvement of antifouling property of the membrane. PES/HNTs-MPC membranes were found to be more hydrophilic, having higher water flux than bare membranes. Zeng *et al.* (2016b) fabricated novel polyvinylidene fluoride (PVDF) nanofiltration membranes by using 3-aminopropyltriethoxysilane (APTES) grafted HNTs and investigated the dye and heavy metals rejection performance and adsorption capacity of membranes. APTES grafted HNT improved the adsorption capacity and rejection performance of membranes with increased stability and reusability.

Before these studies, PSf, PES and PVDF were tested as polymers at the membrane production stage; characterization studies and filtration experiments of the produced membranes were performed. Membranes containing PSf showed the best results, compared to other polymers (Pasaoglu *et al.* 2016). Therefore, the results of all characterization and filtration experiments given within the scope of the experiment are given as the results of PSf containing membranes. Also, membranes containing HNT were produced within the scope of the TÜBİTAK project. In dye treatment, both HNTs' adsorption property and HNTs' hydrophilic properties on the membrane surface were used to increase the flux and increase dye removal (Ormancı-Acar *et al.* 2018). We know that HNTs are hydrophilic and PSf is hydrophobic. When other publications in the literature are examined, as a result of the addition of HNT, it was observed that the contact angle of the membranes increased. This indicates that the membrane is more hydrophilic. Therefore, HNT is used in this article. The agglomeration size of HNT was adjusted in two ways. The 63 μm agglomeration HNTs and 5 μm agglomeration HNTs were produced. The HNT dimensions produced and processed by Esan group were selected from 5 to 63 μm, and the results of the growth of the dimensions were compared. It was observed that HNT was not distributed well and caused agglomeration at high dimensions. Furthermore, when the production of membranes and the construction of membrane modules were considered, it was considered appropriate to produce flat sheet membranes. Additionally, considering the volume/area ratio and the location of the pilot plant, the flat sheet membranes were deemed more advantageous compared to the tubular membrane, as the flat sheet membranes have been used in the scope of this experiment. In the literature, reactive dyes are generally used in the textile industry. Different molecular weights of the dyes selected in this study showed differences in both permeability and removal efficiency results. Besides, if one of the dyes is reactive and the other is reactive, the differences will be reported.

In this study, when the flat sheet HNTs/PSf nanocomposite ultrafiltration (UF) membranes were fabricated, the most important is that using the phase inversion method for the production. Also, as many authors have previously worked with $TiO_2$ added membranes, HNT doped membranes have been produced as an innovative feature of this experiment. The effects of different HNT sizes and ratios on the overall membrane performance were investigated in detail, by determining morphology and dye filtration performances of membranes. The originality of this work is to show the importance of HNT size for nanocomposite membrane fabrication and also the effects of HNT incorporation on UF membrane performance. HNT size is important since HNT is a natural nanotube that has cylindrical, hollow and open-ended structure and low cost. Furthermore, it has a high surface area and fine particle size. Moreover, it can be composed of a double layer of aluminum, silicon, hydrogen and oxygen and it is assumed that the hydroxyl groups on the surface may enhance the flux values of membranes. Also, it may affect the dispersion of HNTs in the membrane matrix. The effects of HNT on dye rejection, pH/temperature stability and surface properties such as charge, hydrophilicity, pore size and mechanical strength were also explored in detail.

## MATERIAL AND METHODS

### Chemicals

Polysulfone (PSf, Udel® P-2700 NT LCD) was used as a polymer. HNT was supplied from EsanNANO Group (Turkey) as 63 μm average size. To obtain 5 μm sized HNT, the Netzsch laboratory granulation and separation system was used. In this system, HNTs were milled by colliding with each other and separated by using a cyclone system that applied pressure up to 7 bars. The average HNT size after treatment was measured as 5 μm.

N-Methly 2-pyrolidinone (NMP), which was a solvent, was bought from Ashland (USA). Reactive Orange (Mw: 617.54 g/mol) was purchased from Sigma-Aldrich for preparing aqueous salt and dye solutions to determine membrane flux and rejection performance. Setazol Red (Mw: 1,463.00 g/mol) was supplied by chemicals producers (Turkey). The dyes are reactive.

## Membrane fabrication

Bare and nanocomposite membrane solutions included 16 wt.% PSf, 84 wt.% NMP and the different ratios of HNTs (0.0–0.63–1.88–3.13–6.30 wt%) were added to the polymer solution as shown in Table 1. HNT in NMP was first ultrasonicated. Then PSf was added slowly to the HNT containing solution and mechanically mixed for 48 h at 60 °C at 400 rpm until a homogeneous solution was obtained. The prepared solutions were cast on the nonwoven support layer in the lab-scale by using the phase inversion method. In this study, a range of membranes with varying thickness was produced. A membrane with a thickness of 130 µm was chosen because it produced better results than other produced membranes. As a result, the knife thickness was adjusted to 130 µm. The membrane casting was performed at room temperature and the coagulation bath temperature was kept at 25 °C. The fabricated bare and nanocomposite membranes were stored for one week at 4 °C. Membranes were denoted M0, M1, M2, M3 and M4 according to their HNT content which were 0.0–0.63–1.88–3.13–6.30 wt%. All HNT concentrations were applied to different HNT sizes.

## Membrane performance determination

Membrane performance tests for permeability and dye removal were determined using the Sterlitech (HP4750 models) dead-end filtration system. The effective membrane area of the dead-end filtration system is 14.6 $cm^2$.

**Table 1** | The composition of casting solution for 5 and 63 µm agglomeration size of HNT

| Membrane ID | PSf content (wt.%) | HNT content (wt.%) | NMP content (wt.%) |
|---|---|---|---|
| M0 | 16.00 | 0.00 | 84.00 |
| M1 | 16.00 | 0.63 | 83.37 |
| M2 | 16.00 | 1.88 | 82.12 |
| M3 | 16.00 | 3.13 | 81.87 |
| M4 | 16.00 | 6.30 | 77.70 |

Before filtration experiments, membranes were compacted for 30 min at 5 bars to obtain stable membrane performance. After compaction, pure water was filtered through the membrane under three different pressures which were 1, 1.5 and 2 bar. Membrane permeability was determined according to Equation (1) given below and rejection of the membrane was determined according to Equation (2) given below:

$$P = J/\Delta P \tag{1}$$

where P: Permeability ($l/m^2$ h.bar), J: Flux ($l/m^2$ h), $\Delta$P: Pressure (bar)

$$R = 1 - (Cp/Cf) \tag{2}$$

where R: Rejection (%), Cp: Permeate concentration, Cf: Feed concentration.

Dye filtration experiments were performed with Setazol Red and Reactive Orange. Synthetic dye solution concentrations were adjusted to 100 mg/L. The reason for choosing synthetic dye concentration is 100 mg/L because dye concentrations close to 100 mg/L were preferred in the previous studies in the literature, and when the dye concentrations of real wastewater were examined, there was a concentration close to 100 mg/L. Dye filtration tests were performed under 2 bar for 1 h. After filtration, permeate was collected for color removal performance determination by using UV spectroscopy (Hach Lange). UV wavelength was chosen as 520 nm for Setazol Red and as 493 nm for Reactive Orange. The zeta potential values of dye solutions were measured with the Malvern Zetasizer nanoseries (Nano-Z) instrument at pH of 7.0 and it was found as −30 mV for Reactive Orange and −40 mV for Setazol Red.

## Membrane characterization

The casting solution was characterized by AND-Vibro Viscometer to see the effects of HNT blending. Membrane morphology and surface properties were determined by thickness, zeta potential, contact angle, pore size, and scanning electron microscope (SEM) analyses. Thickness was performed by Mitutoyo Digital Micrometer. Zeta potential analysis was performed by Anton Parr electrokinetic analyzer. Surface hydrophilicity of membranes was measured with KSV Attension–Theta model contact angle equipment. Six random locations for each membrane sample were used

and average values were reported to minimize the experimental error. A dynamic mechanical analyzer (DMA) (SII Nanotechnology) was used for the mechanical properties of membranes. Pore size measurements were done by Quantachrome 3G Porometer. SEM (FEI–Quanta Feg 250 model) analysis was performed to determine the surface and cross-section morphologies of membranes. The molecular weight cut off (MWCO) analysis is an essential part of membrane performance testing. Molecular weight cutoff values of membranes were determined by GPC-HPLC (Shimadzu). In this part, the molecular weight is prepared from stock chemicals at the concentration appropriate for the measurement range of the GPC-HPLC device. Molecular weights of polyethyleneglycol (PEG) 4,400, 10,000, 35,000 and 100,000 Da were selected as stock chemicals. 1 mL of GPC-HPLC analysis was taken from the filtrate outlet by putting 50 mL of the stock solution into the filtration system. The permeate and samples were collected and measured with the GPC-HPLC. This performance test was repeated for each membrane, and the obtained filtrates were read from the GPC-HPLC device.

### Halloysite nanotube (HNT) characterization

HNT was characterized by means of chemical, mineralogical and morphological analyses, surface area measurement and particle size analysis. X-ray fluorescence (XRF) spectrometer using PANalytical (Axios) was used to determine the elemental composition of HNTs. Super Q+ program was used for quantitative determination. Possible impurities in HNT structure were determined by X-ray diffraction analysis (XRD) using PANalytical (X'Pert Powder). The morphology of HNT was determined by using Field Emission Gun Scanning Electron Microscope (FE-SEM- JSM 7000F) and Transmission Electron Microscope (TEM-Tecnai G2 F30). Also, the cation exchange capacity was determined by the methylene blue method to find the ion exchange amount. In this method, halloysite is mixed with the methylene blue solution in certain proportions and the pigment adsorption of the mineral is measured. Surface area analysis was done according to Brunauer–Emmett–Teller (BET) theory, the gas adsorption measurement was made with the Gemini VII (Mikromeritics). Accordingly, the surface area occupied by the particles was determined. This analysis was conducted using a sedigraph (Micromeritics/Sedigraf III). The device gives the size distribution of particle by collapsing particles in front of the X-Ray bunch for particle size analysis.

## RESULTS AND DISCUSSION

### Properties of HNT

HNTs were analyzed by XRF, BET, average HNT size and cation exchange capacity. Outputs of the XRF spectrometer are summarized in Table 2. The amount of $Al_2O_3$ for 5 μm sized HNT was found to be as high as in 63 μm sized HNT. It can be said, therefore, that a decrease in size did not affect the chemical composition of HNT. According to BET results (Table 3), the specific surface area of HNTs enhanced from 79.7 $m^2/g$ to 100.74 $m^2/g$ for 63 and 5 μm sized HNT, respectively. Additionally, the cation exchange capacity increased from 19.24 meq/100 g to 24.42 meq/100 g for 63 and 5 μm sized HNT, respectively.

FE-SEM and high-resolution transmission electron microscopy (HRTEM) were used for the structure and morphology of HNTs. FE-SEM (SEM: FEG-SEM Zeiss Leo Supra 35VP) images were obtained from different points of the HNT structures. Referring to Figure 1, it is understood that the dispersion is homogeneous and the cylindrical structure of the HNT nanotubes is preserved. Figure 1 represents the SEM of 63 or 5 μm HNTs. Figure 2 represents the SEM and TEM of 5 μm HNT.

**Table 2** | Chemical analysis of HNTs

| Component, % | 63 μm sized HNT | 5 μm sized HNT |
|---|---|---|
| Loss on ignition (LOI) | 15.38 | 16.81 |
| $SiO_2$ | 44.68 | 44.00 |
| $Al_2O_3$ | 38.85 | 37.59 |
| $Fe_2O_3$ | 0.62 | 0.69 |
| $TiO_2$ | 0.06 | 0.14 |
| CaO | 0.05 | 0.12 |
| MgO | 0.14 | 0.29 |
| $Na_2O$ | 0.15 | 0.06 |
| $K_2O$ | 0.04 | 0.29 |

**Table 3** | Characterization results of HNTs

| | | 63 μm sized HNT | 5 μm sized HNT |
|---|---|---|---|
| Average size (μm) (*SediGraph*) | $d_{10}$ | 0.92 | 0.08 |
| | $d_{50}$ | 9.92 | 0.21 |
| | $d_{90}$ | 57.88 | 4.61 |
| Specific surface area (*BET*) | $m^2/g$ | 79.70 | 100.74 |
| Cation exchange capacity (*CEC*) | meq/100 g | 19.24 | 24.42 |

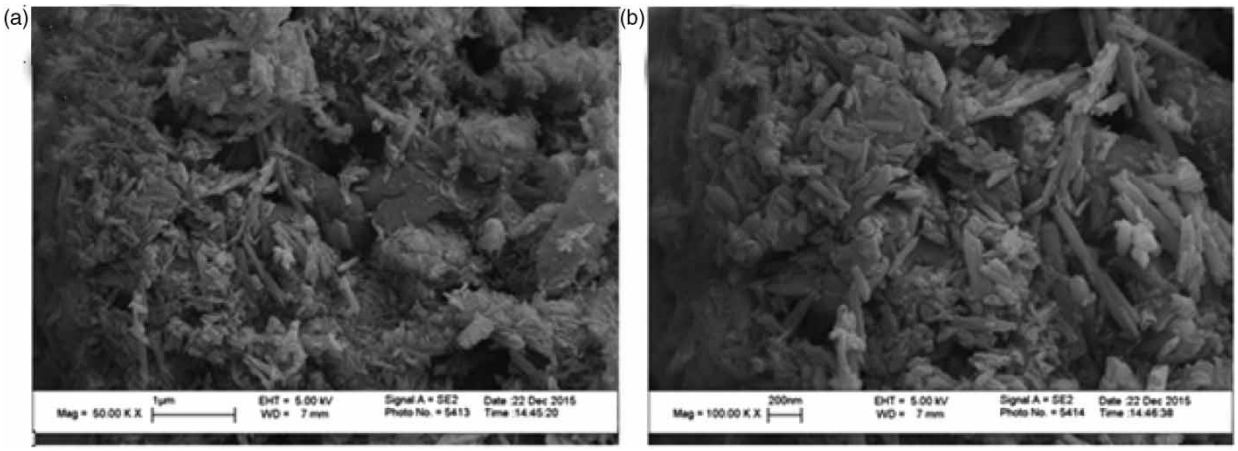


**Figure 1** | SEM images of HNT (a: 5 μm after milled HNTs, b: 63 μm original HNTs).

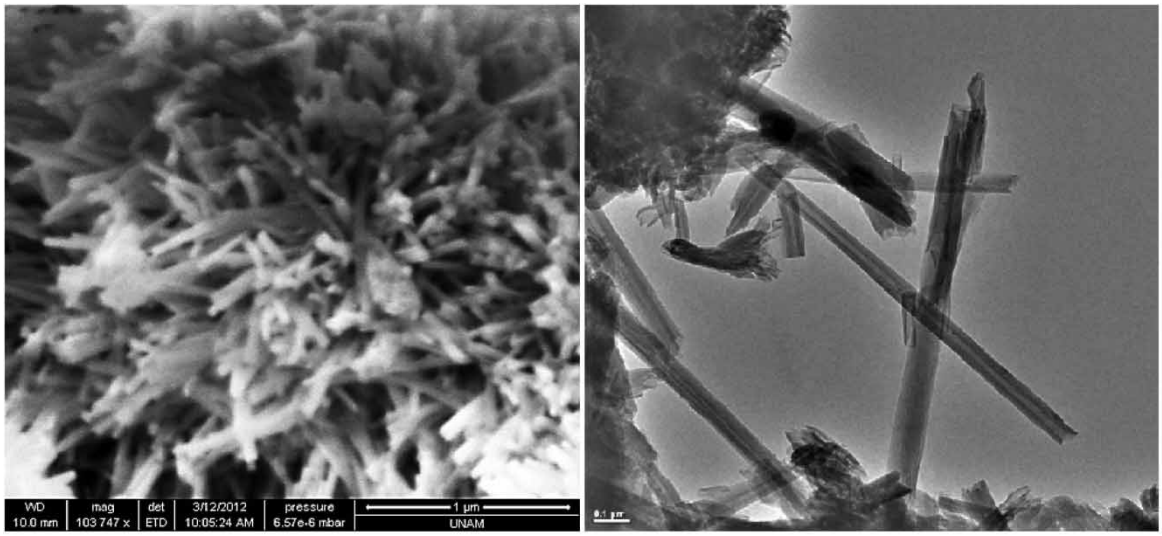


**Figure 2** | SEM and TEM images of 5 μm after milled HNT.

## Structural properties of bare and nanocomposite membranes

Characterization results of all membranes are given in Table 4. Because of the addition of HNT to the membrane, the viscosity of polymer solution enhanced from 0.53 to 0.65 Pa.s. As stated in Hendrix *et al.* (2013), the most important characterization is viscosity for phase inversion. When the viscosity of the cast solution is high, during the casting process, the diffusion between solvent and non-solvent in the coagulation bath is decelerated. As a result, macrovoid generation is prevented and denser membranes are fabricated. Sengur *et al.* (2015) used MWCNTs (multiwalled carbon nanotube) for the fabrication of PES hollow fiber membranes and viscosity measurements showed that the addition of MWCNT increased the viscosity of casting solution from 6 Pa.s to nearly 9 Pa.s for pristine membranes and 0.8% of MWCNT membranes, respectively. CNT and HNT can be considered similar materials because of their nanotube property. In this context, it can be said that CNT's and HNT's addition effects on viscosity are comparable. In our case, the addition of HNT also increased the viscosity from 0.53 Pa.s to 0.65 Pa.s as can be seen in Table 4.

When HNT concentration increased, at pH 7, the highest negative values were obtained from the membrane surface. As can be seen in Table 4, for pristine membranes, zeta potential value was measured as −27.3 mV but with the addition of HNT, zeta potential value reached −46.8 mV. Pasbakhsh *et al.* (2013) studied zeta potential variations of

**Table 4** | Characterization of membranes

| | 5 μm HNT | | | | 63 μm HNT | | | |
|---|---|---|---|---|---|---|---|---|
| Membrane type | Viscosity (Pa.s) | Zeta potential (mV) | Contact angle (°) | Youngs modulus (MPa) | Viscosity (Pa.s) | Zeta potential (mV) | Contact angle (°) | Young's modulus (MPa) |
| M0 | 0.53 | −27.3 | 80.60 ± 3.11 | 41.6 ± 2.1 | 0.53 | −27.3 | 80.60 ± 3.11 | 41.6 ± 2.1 |
| M1 | 0.61 | −42.8 | 74.70 ± 2.86 | 68.7 ± 3.4 | 0.57 | −31.8 | 92.40 ± 1.37 | 71.6 ± 3.6 |
| M2 | 0.61 | −44.1 | 90.40 ± 1.54 | 106.0 ± 5.3 | 0.57 | −28.0 | 91.10 ± 2.47 | 90.5 ± 4.5 |
| M3 | 0.62 | −45.0 | 86.00 ± 0.95 | 107.7 ± 5.4 | 0.59 | −28.0 | 87.30 ± 1.38 | 65.0 ± 3.3 |
| M4 | 0.65 | −46.8 | 78.20 ± 0.49 | 120.8 ± 6.1 | 0.53 | −34.4 | 70.00 ± 0.03 | 57.7 ± 2.9 |

HNT in water pH range between 1.5 to 12. Zeta potential results obtained in the study showed that HNT has a negative charge in general and the negativity of charges increased in alkaline conditions. Ghanbari *et al.* (2015) computed the zeta potential of pristine and HNT embedded membranes and have seen that zeta potential values of membranes decreased from 2.5 mV to ∼−25 mV when pH was changed from pH 4 to pH 9. In our study, it can be seen that the results of zeta potential experiments showed a similar trend. Table 4 shows that the 5 μm sized HNT incorporated membrane's surface charge was more negative than the 63 μm sized HNT incorporated membrane's surface charge. For instance, zeta potential values of M1 membranes are −42.8 mV and −31,8 mV, respectively, for 5 and 63 μm sized HNTs.

The contact angle of membranes containing 5 μm HNT is generally decreased, but it has been observed that the contact angle increases with changing surface roughness due to high concentrations of agglomerations; the hydrophilicity was increased by the addition of the HNT. According to Wang *et al.* 2017, as a result of adding nanotubes, membrane was more hydrophilic than without nanotubes (Wang *et al.* 2017). Moreover, when the contact angles of the membranes with HNT concentrations are compared; after the HNT concentration exceeded 3.13 wt%, the contact angle decreased as a result of both agglomerations of HNT and increased surface roughness. It is well-known that in addition to chemical structure, surface topography and roughness also play a critical role in water contact angle on membrane surfaces.

Young's modulus is an important parameter for the determination of the mechanical stabilities of membranes. In a recent study, Lai *et al.* (2015) fabricated PVDF/nanoclay nanocomposite membranes by applying different casting conditions such as air retention time and bath temperature. The incorporation of nanoclay into the membrane matrix increased the mechanical properties of membranes by 76%. It can be seen that nanoclay incorporation into the membrane matrix had a positive effect on Young's modulus. According to our study, higher Young's modulus values were obtained for nanocomposite membranes. As the HNT ratio increased, Young's modulus values increased for membranes containing 5 μm sized HNT. Young's modulus values first increased then decreased for 63 μm sized HNT which can be due to the additional agglomeration of HNT at bigger particle sizes.

Samples from membranes filtered with different molecular weight polyethylene glycol (PEG) were analyzed using the GPC-HPLC device. Molecular weight cutting values (MWCO) of membranes were calculated with the obtained results. According to MWCO analysis, the range of membranes produced is 10,000–100,000,000 Da. This indicates that the membranes are ultrafiltration membranes. Besides, consistency was observed between MWCO values and transmittance values. As the MWCO value increases, the permeability values of the membranes are expected to increase.

The average pore size range of the ultrafiltration membranes is 0.01–0.1 μm. The largest pore is the void (the lowest pressure generating current) is defined as the 'bubble point'. As a result of measuring all pores on the same sample, first wet and then dry, a gap is created in all pores. Various flow-related pore diameter parameters, pore diameter distributions and gas permeability can be calculated from the completed datasets. As a result of these calculations, all membranes according to mean pore size results, pore size M0 was 0.09 μm and the other membranes pore size were 0.04 μm.

SEM images of membranes containing HNTs of 5 and 63 μm in size are shown in Table 5. The membranes had finger-like structures as can be seen from cross-sectional SEM images. When the ratio of HNT increased, the finger-like structure of the membrane became more dominant. This may increase water permeability since water can find a way to percolate through the membrane matrix easily. In

**Table 5** | Cross-sectional and surface SEM images of M0, M1, M2, M3, M4 membranes

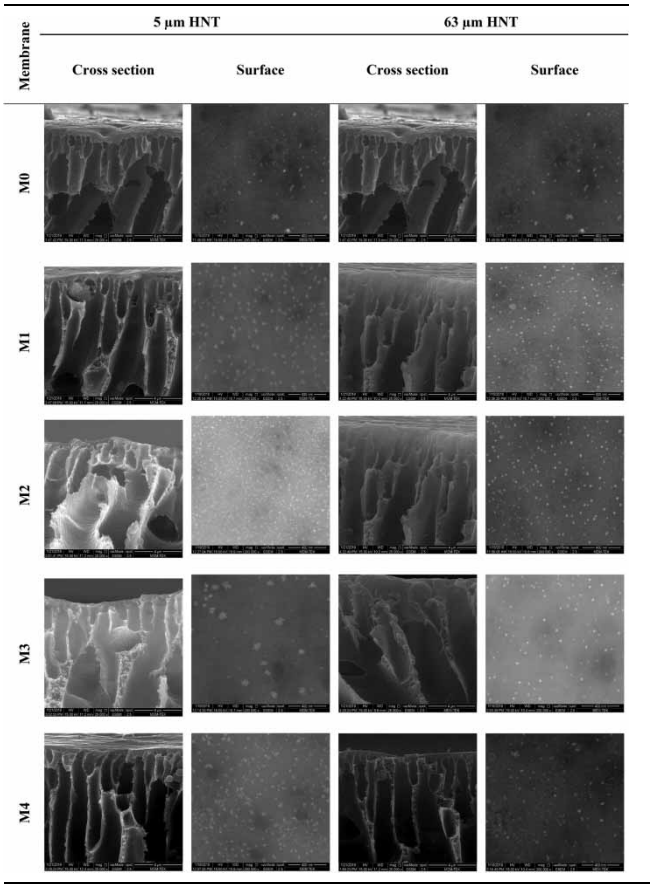


a recent study, Zeng *et al.* (2017) used modified HNTs with dopamine and they fabricated PVDF nanocomposite membranes by using different ratios of functionalized HNT. According to SEM images, there were no particular changes between the surface morphology of pristine PVDF membrane and HNT incorporated membranes. On the other hand, the addition of D-A-modified HNT resulted in the gradual increase of microcavities in membrane structure and formed more channel-like structures in the sub-layer, similar to our cross-section SEM images.

## Filtration results

In this part, three parallel experiments were done for measuring pure water permeability. Referring to Figure 3, pure water permeability is increased compared to 5 μm HNT added membranes and pure membrane. However, when the concentration reached a certain level, decreases in pure water permeability due to HNT agglomeration were observed. In the same case, pure water permeability is reduced when 63 μm HNT added membranes and pure membranes are compared. However, it was observed that pure water permeability increased when the HNT concentration was increased. As can be seen from Figure 3, a certain trend cannot comply with 63 μm sized HNT. It is thought that inconsistencies in permeability are seen as a result of the fact that 63 μm sized HNT is more agglomerated and collected in a certain part of the membrane and is not completely distributed in the membrane. Zeng *et al.* (2016b) stated that HNT tends to agglomerate due to HNT's high length to diameter ratio. This situation is the main disadvantage of HNT. Therefore, the decrease in permeability with increasing HNT ratio may be ascribed to the agglomeration of HNT in the membrane's matrix. Overall, 5 μm sized HNT has higher permeability than 63 μm sized HNT.

## Dye removal performances of fabricated membranes

### Effects of HNT size and concentration on dye removal performance

Two different types of dye solutions were prepared for the dye removal tests which were Setazol Red and Reactive Orange dyes. Molecular weight of Setazol Red (MW = 1,463 g/mole)

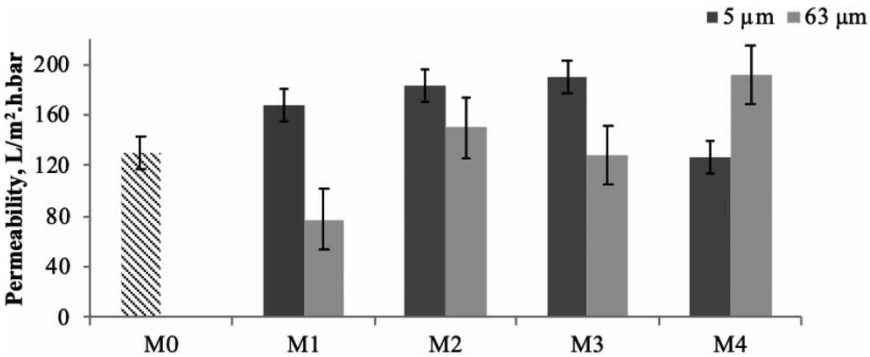


**Figure 3** | Pure water permeability of 5 and 63 μm of HNT membranes.

is higher than reactive orange (MW = 617.54 g/mole). Two dye solutions were filtered separately through pristine and HNT incorporated membranes.

Except for M2 membranes, incorporation of different sized HNT was led to lower flux compared to pristine membrane. However, increasing the ratio of HNT (except M2) resulted in increased flux values. 5 μm sized HNT's surface area is greater than 63 μm HNT's surface area which may have resulted in better flux values than high sized HNT. When pristine membrane and membranes containing 5 μm sized HNT are compared with each other, the M0 membrane has the highest flux value. When pristine and nanocomposite membranes with 63 μm sized HNT were compared, the M2 membrane has the highest flux value and the M1 membrane has the lowest flux value (Figure 4).

According to Figure 4, when pristine membrane and membranes containing 63 μm sized HNT compare with each other, the M1 membrane has the highest efficiency for removing dye solution. The removal efficiency of membranes decreases as a result of increasing HNT. It is believed to be caused by a pin-hole problem according to the finger-like morphology at high HNT content. For membranes containing 5 μm HNT, the M1 membrane has the highest removal efficiency value and the M0 membrane has the lowest efficiency value. After a certain concentration of HNT, the removal efficiency decreases owing to the resistance of HNT in the membrane pore (Figure 4).

In recent research, Nikooe (Nikooe & Saljoughi 2017) fabricated PVDF/Brij-58 blend nanofiltration membranes. They used Brij-58 surfactant as a hydrophilic additive. They tested membrane performance by water and synthetic dye solutions flux. For fouling tendency tests, they also used BSA (bovine serum albumin). For dye performation tests, reactive red 141(RR141) was used and colored feed solutions concentration was 15 ppm. After dye filtration, the efficiency results were obtained and the average retention of reactive dye was 90% (Nikooe & Saljoughi 2017). In our study, we also used the reactive type of dyes and the highest retention that we obtained was 74%. Our membranes can be classified as ultrafiltration membranes. Although UF membranes are not expected to remove high dye solutions under normal conditions, in this study UF membranes showed significant dye removal performance. High removal efficiency is caused due to the adsorption capacity of HNT in the membrane matrix. Additionally, electrostatic repulsion of dyes from the membrane surface may be another reason since both HNT and dye solution has the same charge. When 63 and 5 μm compare with each other for the filtration of Reactive Orange dye solution, all 5 μm have high and stabile flux values. After 1.88% of HNT content, 63 μm is better than 5 μm owing to the resistance of HNT in the membrane pores (Figure 5). The results of the filtration Reactive Orange rejection are shown in Figure 5.

When we sum up all the results above, it can be said that, when the molecular weight of dye is high, the membrane retains the dye more easily than the dye which has a smaller molecular weight. Because of that reason, the flux is low but removal efficiency is high for the high molecular weight of dye. When the molecular weight of the dye is small, the dye can be filtered through membrane pores more easily. Therefore, flux is high and removal efficiency is low. Consequently, when we consider all the results we obtained, it can be seen that 5 μm of HNT incorporated membranes have better results.

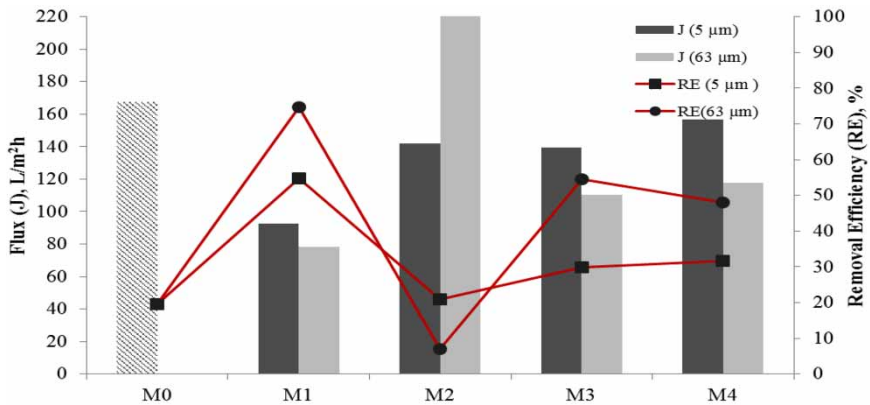


**Figure 4** | Setazol Red dye flux and removal efficiency of membranes.

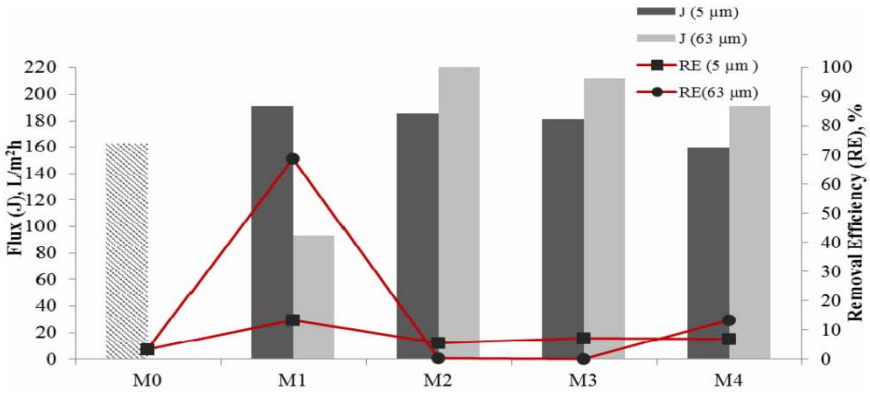


**Figure 5** | Reactive Orange dye flux and removal efficiency of membranes.

## Effects of different pH and temperature on membrane dye removal performance

After dye filtration and removal experiments, different pH (pH: 4–8–11) and temperature (T:15 °C −25 °C −40 °C) experiments were conducted. According to characterization and performance results, pristine (M0) and M1 membranes with 5 µm sized HNT were selected. According to M0 membrane, pure water fluxes were 70.8 L/m$^2$.h, 80.1 L/m$^2$.h and 113.2 L/m$^2$.h for 15 °C −25 °C −40 °C, respectively. Also, according to M1 membrane, pure water fluxes were 75.7 L/m$^2$.h, 100.5 L/m$^2$.h and 118.6 L/m$^2$.h for 15 °C, −25 °C, and −40 °C, respectively. It can be seen that fluxes enhanced with increasing temperature which is generally expected for polymeric membranes. The flux of membranes can be increased by increasing temperature. It depends on water viscosity which is decreased by increasing temperature (He *et al.* 2008). According to the equation of Agashichev and Lootahb, when the viscosity is decreased, the water flux is increased (Agashichev & Lootahb 2003). The equation is that if the viscosity of the solution decreased, the solution of temperature could be raised while the diffusion coefficient is increasing. The mass transfer resistance affected by changing viscosity and diffusion coefficient (Koyuncu & Topacik 2003). As a result of increasing temperature, the permeate flux increases and the removal of dye solution decreases. Given all this, the temperature affects dye absorption. Higher temperature tends to distribute dyes more evenly between the solution and membrane phases, which means less selective partitioning, and as a result, lower rejection found similar trends for permeability increase as temperature increased (Tsai *et al.* 2006; Liu *et al.* 2017). In their study, the dye solution permeates flux enhances from 95 L/m$^2$.h to 138 L/m$^2$.h, as the operating temperature changes from 20 °C to 95 °C at 0.3 MPa applied pressure. As it can be seen from pure water fluxes, M1 membrane flux values are higher than the M0 membrane flux values, as obtained before in HNT incorporated membranes.

Setazol red dye solution filtration results at three different pH and temperature values were given in Figure 6. According to zeta potential analysis results, the pH where the surface negativity is highest is around 8 for the M0 and M1 membranes. So that the highest flux values were obtained at pH 8. Figure 6 is shown that the M1 membrane showed better performance than pristine membrane at acidic and basic conditions. This may be since the M1 membrane has a higher resistance to pH variations due to HNT content. At pH 11, M1 membrane flux is twice as high as the M0 membrane. Since the application of the majority of reactive dye in the textile industry is done at higher pH values, therefore wastewater will have high pH values. It is very important to obtain high flux in HNT addition membranes at pH 11.

Setazol Red dye removal efficiencies were shown in Figure 6. From a general point of view, the M1 membrane (HNT incorporated membrane) has better removal performance for each pH and temperature point. This can be attributed to the presence of HNT in the M1 membrane matrix. According to Ghanbari *et al.*, an increase in flux was observed due to the gap formed at the interface between HNT and polymer. Therefore, water flow channels are formed by the polyamide matrix (Ghanbari *et al.* 2016). Also, the cylindrical, hollow and open-ended structure of HNTs could promote the water passage (Ghanbari *et al.* 2015).

The results of the experiments performed with different temperatures and pH values conducted with Reactive Orange dye solutions are given in Figure 7. According to zeta potential analysis results, the pH where the surface

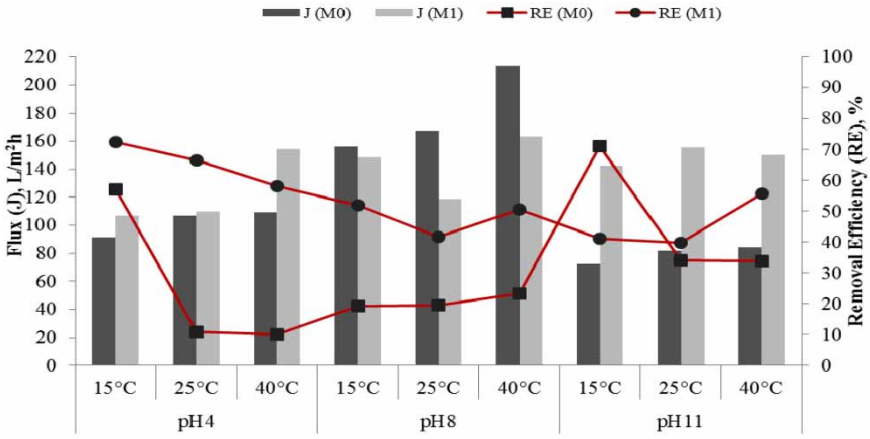


**Figure 6** | Setazol Red dye flux and removal efficiency of M0 and M1 membranes at three different temperatures and pH values.

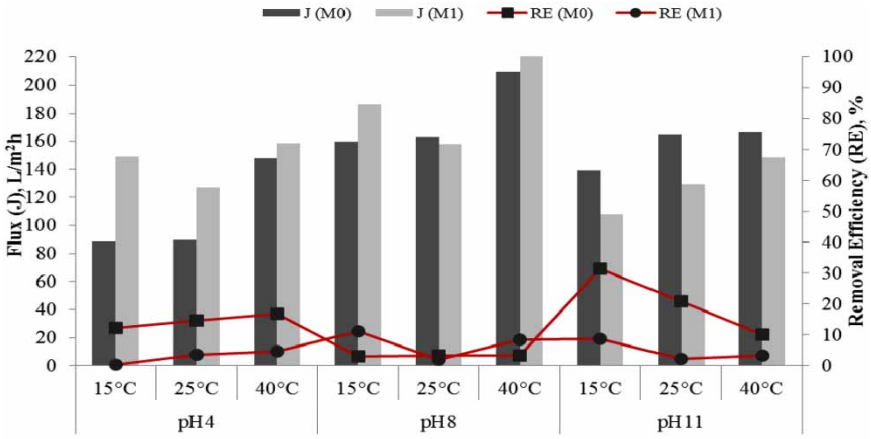


**Figure 7** | Reactive Orange dye flux and removal efficiency of M0 and M1 membranes at three different temperatures and pH values.

negativity is highest is around 8 for the M0 and M1 membranes. So that the highest flux values were obtained at pH 8. As shown in Figure 7, HNT incorporated the M1 membrane gave a higher flux value at acidic and neutral pH values. However, the dye removal efficiency in the M1 membrane was higher at neutral pH. The obtained results for Reactive Orange dye are not better than Setazol Red removal efficiency values. This may be because the Reactive Orange dye has a smaller molecular weight than Setazol Red. Therefore, the Reactive Orange dye can be retained from the membrane less than the Setazol Red dye.

## CONCLUSIONS

HNT incorporated polysulfone nanocomposite ultrafiltration membranes that were fabricated in this study. For this purpose, two different HNT sizes (5 and 63 μm) were chosen and five different HNT ratios (0, 0.63, 1.88, 3.13, 6.30 wt %) were used. Fabricated membranes were characterized in terms of morphology, surface charge and hydrophilicity, mechanical properties, membrane performance, such as water permeability and dye filtration, at different HNT ratios, as well as three different pH and temperature values. HNT size had effects on membrane properties. The membranes having 5 μm sized HNT had more negative surface and higher mechanical strength than 63 μm sized HNT. Permeability values and setazol red flux values are higher in membranes having 5 μm sized HNT than membranes having 63 μm sized HNT. Also, the reactive orange flux values of membranes fabricated with 63 μm sized HNT are higher than those with 5 μm sized HNT. This may be due to the electrostatic interactions between the dye molecules and the membrane surface

charge and therefore different sieving coefficients. Another important parameter is the concentration of HNT which determines dispersibility. High HNT concentrations have led to poor filtration performance, often due to defects in the membrane structure (visible from Figures 3 and 4). When all results are taken into consideration, the addition of 1.88 wt.% of 5 μm sized HNT can be suggested in terms of membrane performance. In future studies, the pilot-scale membrane will be produced with the selected HNT size and HNT concentration as a result of this study. Then, both synthetic wastewater (containing dye and salt) and real textile wastewater will be passed through these membranes and the results will be examined.

## ACKNOWLEDGEMENTS

This work was supported by The Scientific and Technological Research Council of Turkey (TUBİTAK) under project numbers of 113Y350, 113Y370, 113Y371 and 113Y372. B.K. (PhD student) did the experiments and wrote the article. M.A. (PhD student) did the experiments and revised the article. T.O.A. (Doctor) did the experiments and revised the article. T.T. (Doctor) did SEM characterization analysis. D.Y.I. (Associate Professor) revised the article. S.U. (Associate Professor) revised the article and is project manager. Y.Z.M. (Professor) revised the article. T.U.D. (MSc and R & D Manager) did HNT characterization analysis. I.K. (Professor) revised the article and is project manager.

## DATA AVAILABILITY STATEMENT

All relevant data are included in the paper or its Supplementary Information.

## REFERENCES

Agashichev, S. P. & Lootahb, K. N. 2003 Influence of temperature and permeate recovery on energy consumption of a reverse osmosis system. *Desalination.* **154**, 253–266.

Baker, R. W. 2004 *Membrane Technology and Applications*, 2nd edn. Wiley: Academic Press, CA, USA, pp. 262–272.

Celik, E., Park, H., Choi, H. & Choi, H. 2011 Carbon nanotube blended polyethersulfone membranes for fouling control in water treatment. *Water Res.* **45**, 274–282.

Chen, Y., Zhang, Y., Liu, J., Zhang, H. & Wang, K. 2012 Preparation and antibacterial property of polyethersulfone ultrafiltration hybrid membrane containing halloysite nanotubes loaded with copper ions. *Chem. Eng. J.* **210**, 298–308.

Choi, J. H., Jegal, J. & Kim, W. N. 2006 Fabrication and characterization of multi-walled carbon nanotubes/polymer blend membranes. *J. Memb. Sci.* **284**, 406–415.

Crock, C. A., Sengur-Tasdemir, R., Koyuncu, I. & Tarabara, V. 2017 High throughput catalytic dechlorination of TCE by hollow fiber nanocomposite membranes with embedded Pd and Pd-Au catalysts. *Separ. Purif. Technol.* **179**, 265–273.

de Paiva, L. B., Morales, A. R. & Valenzuela-Díaz, F. R. 2008 Organoclays: properties, preparation and applications. *Appl. Clay Sci.* **42**, 8–24.

Dilaver, M., Murat-Hocaoglu, S., Soydemir, G., Dursun, M., Keskinler, B., Koyuncu, I. & Agtas, M. 2018 Hot wastewater recovery by using ceramic membrane ultrafiltration and its reusability in textile industry. *J. Clean. Prod.* **171**, 220–233.

Ellouze, E., Tahri, N. & Amar, R. B. 2012 Enhancement of textile wastewater treatment process using nanofiltration. *Desalination.* **286**, 16–23.

Ghanbari, M., Emadzadeh, D., Lau, W. J., Lai, S. O., Matsuura, T. & Ismail, A. F. 2015 Synthesis and characterization of novel thin-film nanocomposite (TFN) membranes embedded with halloysite nanotubes (HNTs) for water desalination. *Desalination.* **358**, 33–41.

Ghanbari, M., Emadzadeh, D., Lau, W. J., Riazi, H., Almasi, D. & Ismail, A. F. 2016 Minimizing structural parameter of thin-film composite forward osmosis membranes using polysulfone/halloysite nanotubes as membrane substrates. *Desalination.* **377**, 152–162.

He, Y., Li, G., Wang, H., Zhao, J., Su, H. & Huang, Q. 2008 Effect of operating conditions on separation performance of reactive dye solution with membrane process. *J. Memb. Sci.* **321**, 183–189.

Hendrix, K., Vaneynde, M., Koeckelberghs, G. & Vankelecom, I. F. J. 2013 Synthesis of modified poly(etheretherketone) polymer for the preparation of ultrafiltration and nanofiltration membranes via phase inversion. *J. Memb. Sci.* **447**, 96–106.

Koyuncu, I. 2002 Reactive dye removal in dye/salt mixtures by nanofiltration membranes containing vinylsulphone dyes: effects of feed concentration and cross flow velocity. *Desalination.* **143**, 243–253.

Koyuncu, I. & Topacik, D. 2003 Effects of operating conditions on the salt rejection of nanofiltration membranes in reactive dye/salt mixtures. *Separ. Purif. Technol.* **33**, 283–294.

Lai, C., Groth, A., Gray, S. & Duke, M. 2015 Impact of casting conditions on PVDF/nanoclay nanocomposite membrane properties. *Chem. Eng. J.* **267**, 73–85.

Liu, M., Chen, Q., Lu, K., Huang, W., Lu, Z., Zhou, C., Yu, S. & Gao, C. 2016 High efficient removal of dyes from aqueous solution through nanofiltration using diethanolamine-modified polyamide thin-film composite membranes. *Separ. Purif. Technol.* **173**, 135–143.

Liu, C., Mao, H., Zheng, J. & Zhang, S. 2017 Tight ultrafiltration membrane: preparation and characterization of thermally resistant carboxylic cardo poly (arylene ether ketone)s (PAEK-COOH) tight ultrafiltration membrane for dye removal. *J. Memb. Sci.* **530**, 1–10.

Mokkapati, V. R. S. S., Koseoglu-Imer, D. Y., Yilmaz, N., Ozguz, V. & Koyuncu, I. 2015 Protein mediated textile dye filtration using graphene oxide polysulfone composite membranes. *RSC Adv.* **5**, 71011–71021.

Moslehyani, A., Mobaraki, M., Ismail, A. F., Matsuura, T., Hashemifard, S. A., Othman, M. H. D. & Shamsaei, E. 2015 Effect of HNTs modification in nanocomposite membrane enhancement for bacterial removal by cross-flow ultrafiltration system. *React. Funct. Polym.* **95**, 80–87.

Nikooe, N. & Saljoughi, E. 2017 Preparation and characterization of novel PVDF nanofiltration membranes with hydrophilic property for filtration of dye aqueous solution. *Appl. Surf. Sci.* **413**, 41–49.

Ormancı-Acar, T., Celebi, F., Keskin, B., Mutlu-Salmanlı, O., Agtas, M., Turken, T., Tufani, A., Koseoglu-Imer, D. Y., Ozaydın-Ince, G., Ucar-Demir, T., Menceloglu, Y. Z., Unal, S. & Koyuncu, I. 2018 Fabrication and characterization of temperature and pH resistant thin film nanocomposite membranes embedded with halloysite nanotubes for dye rejection. *Desalination.* **429**, 20–32.

Pasaoglu, M. E., Guclu, S. & Koyuncu, I. 2016 Polyethersulfone/polyacrylonitrile blended ultrafiltration membranes: preparation, morphology and filtration properties. *Water Sci. Technol.* **74**, 738–748.

Pasbakhsh, P., Churchman, G. J. & Keeling, J. L. 2013 Characterisation of properties of various halloysites relevant to their use as nanotubes and microfibre fillers. *Appl. Clay Sci.* **74**, 47–57.

Qin, J. J., Oo, M. H. & Kekre, K. 2007 Nanofiltration for recovering wastewater from a specific dyeing facility. *Separ. Purif. Technol.* **56**, 199–203.

Sengur, R., Lannoy, C., Turken, T., Wiesner, M. & Koyuncu, I. 2015 Fabrication and characterization of hydroxylated and carboxylated multiwalled carbon nanotube/polyethersulfone (PES) nanocomposite hollow fiber membranes. *Desalination.* **359**, 123–140.

Sengur-Tasdemir, R., Mokkapati, V. R. S. S., Koseoglu-Imer, D. Y. & Koyuncu, I. 2018 Effect of polymer type on characterization and filtration performances of multi-walled carbon nanotubes (MWCNT)-COOH-based polymeric mixed matrix membranes. *Environ. Technol.* **39**, 1226–1237.

Song, D., Xu, J., Fu, Y., Xu, L. & Shan, B. 2016 Polysulfone/sulfonated polysulfone alloy membranes with an improved performance in processing mariculture wastewater. *Chem. Eng. J.* **304**, 882–889.

Sotto, A., Boromand, A., Zhang, R., Luis, P., Arsuaga, J. M., Kim, J. & Van der Bruggen, B. 2011 Effect of nanoparticle aggregation at low concentrations of $TiO_2$ on the hydrophilicity, morphology, and fouling resistance of PES–$TiO_2$ membranes. *J. Colloid Interface Sci.* **363**, 540–550.

Tsai, H. A., Chen, H. C., Lee, K. R. & Lai, J. Y. 2006 Study of the separation properties of chitosan/polysulfone composite hollow-fiber membranes. *Desalination.* **193**, 129–136.

Turken, T., Sengur-Tasdemir, R., Koseoglu-Imer, D. Y. & Koyuncu, I. 2015 Determination of filtration performances of nanocomposite hollow fiber membranes with silver nanoparticles. *Environ. Eng. Sci.* **32**, 656–665.

Wang, Z., Wang, H., Liu, J. & Zhang, Y. 2014 Preparation and antifouling property of polyethersulfone ultrafiltration hybrid membrane containing halloysite nanotubes grafted with MPC via RATRP method. *Desalination.* **344**, 313–320.

Wang, G., Zhang, H., Wang, J., Ling, Z. & Qiu, J. 2017 In situ synthesis of chemically active ZIF coordinated with electrospun fibrous film for heavy metal removal with a high flux. *Separation and Purification Technology.* **177**, 257–262.

Zeng, G., He, Y., Zhan, Y., Zhang, L., Pan, Y., Zhang, C. & Yu, Z. 2016a Novel polyvinylidene fluoride nanofiltration membrane blended with functionalized halloysite nanotubes for dye and heavy metal ions removal. *J. Hazard. Mater.* **317**, 60–72.

Zeng, G., He, Y., Yu, Z., Zhan, Y., Ma, L. & Zhang, L. 2016b Preparation and characterization of a novel PVDF ultrafiltration membrane by blending with $TiO_2$-HNTs nanocomposites. *Appl. Surf. Sci.* **371**, 624–632.

Zeng, G., Ye, Z., He, Y., Yang, X., Ma, J., Shi, H. & Feng, Z. 2017 Application of dopamine-modified halloysite nanotubes/PVDF blend membranes for direct dyes removal from wastewater. *Chem. Eng. J.* **323**, 572–583.

Zhang, R., Ji, S., Wang, N., Wang, L., Zhang, G. & Li, J. R. 2014 Coordination-driven InSitu self-assembly strategy for the preparation of metal–organic framework hybrid membranes. *Angew. Chem.Int. Ed.* **53**, 9775–9779.

Zuriaga-Agustí, E., Iborra-Clar, M. I., Mendoza-Roca, J., Tancredi, M., Alcaina-Miranda, M. I. & Iborra-Clar, A. 2002 Sequencing batch reactor technology coupled with nanofiltration for textile wastewater reclamation. *Chem. Eng. J.* **161**, 122–128.

First received 8 September 2020; accepted in revised form 21 November 2020. Available online 2 December 2020